applied sciences

MDPI

Article

Advantage of Steerable Catheter and Haptic Feedback for a 5-DOF Vascular Intervention Robot System

Jaehong Woo [1], Hwa-Seob Song [2], Hyo-Jeong Cha [3,*] and Byung-Ju Yi [2,*]

[1] Department of Intelligent Robot Engineering, Hanyang University, 222 Wangsimni-ro, Seongdong-gu, Seoul 04763, Korea; jokers12@nate.com

[2] Department of Electrical and Electronic Engineering, Hanyang University, 55 Hanyangdaehak-ro, Sangnok-gu, Ansan 15588, Korea; surgerybot@hanyang.ac.kr

[3] Department of Medical Device Daegu Research Center for Medical Devices and Green Energy, Korea Institute of Machinery & Materials, 330 Techno sunhwan-ro, Yuga-eup, Dalseong-gun, Daegu 42994, Korea

* Correspondence: chacne@hanmail.net (H.-J.C.); bj@hanyang.ac.kr (B.-J.Y.); Tel.: +82-31-400-5218 (B.-J.Y.)

Received: 29 July 2019; Accepted: 6 October 2019; Published: 14 October 2019

Abstract: Vascular intervention involves inserting a catheter and guidewire into blood vessels to diagnose and treat a disease in an X-ray environment. In this conventional vascular intervention procedure, the doctor is exposed to considerable radiation. To reduce the exposure, we developed a master–slave robot system. A steerable catheter is employed to shorten the task-time and reduce the contact force applied to the vessel walls during catheter insertion. The steerable catheter helps to select a vascular branch; thus, the radiation exposure time for patients is reduced, and perforation in the patient's vessel is prevented. Additionally, the robot system employs a haptic function to replicate the physician's tactile sensing in vascular intervention. In this study, the effectiveness of the steering catheter and haptic function was demonstrated experimentally in comparison with a conventional catheter.

Keywords: vascular intervention; surgical robot; haptic; catheter; steering; master–slave system

1. Introduction

The catheter-based approach is an important and common method for treating vascular and cardiac disease. Application of the catheter-based technique has grown from simple stenting to complex aortic and valve procedures [1–3]. Vascular interventional radiology (VIR) is used to diagnose and treat diseases in the vascular system by using several vascular tools, such as catheters and guidewires. However, because angiography is frequently performed to visualize the arteries and the catheter in the body, operators are exposed to large amounts of radiation [4–9]. Most countries regulate the radiation dose limit for occupationally exposed persons according to the recommendations of the International Commission on Radiological Protection (ICRP). As prescribed by ICRP 103 [10], the effective dose limit for radiation workers is 20 millisieverts (mSv) per year, averaged over 5 years with no more than 50 mSv in any one year. Because of the dose limit, the number of procedures for a year is restrictive. Radiation workers wear radiation protection, such as aprons, collars, glasses, and gloves, but they become stressed owing to the weight of the apron. Additionally, use of gloves is low; thus, doses to the hands are high [5]. Robotic systems are undergoing major development. They need careful clinical evaluation and should be tailored to specific clinical needs. In some cases, e.g., patients with acute coronary syndrome or high-syntax score lesions, special evaluation is needed for applying a robotic system [11–13]. Therefore, a master–slave robotic system for VIR is necessary for minimization of the radiation exposure to operators.

Reducing the radiation doses to the patient and physician is important. If the curvature of the vasculature is large, vascular selection using a catheter takes a long time, and the radiation dose to the

patient is increased. Therefore, to reduce the time needed to select a vascular branch with a catheter, it is necessary to develop a steering catheter whose tip is capable of bending freely according to the curvature of the blood vessel.

Because vascular intervention depends on the physician's tactile sense, haptic function is very important. The physician's movements are determined by using tactile information regarding the contact force between the VIR devices and the blood-vessel wall; thus, the haptic function significantly affects the safety of the patient.

Various robot systems reflect these requirements [14]. To avoid the radiation exposure, the slave robot of the systems is installed on a surgical bed, and an operator controls the slave robot from the master console, which is separated from the bed.

Hansen Medical Co. developed the Magellan robotic system and the Sensei robotic system [15,16]. The Magellan robotic system has a robotic catheter system that controls a guidewire, a sheath, and a robotic catheter for a wide variety of endovascular procedures. The guidewire can be inserted and rotated, and the sheath and the robotic catheter can be not only inserted but also steered in four directions.

The Sensei robotic system has a robotically steerable sheath for intracardiac electrophysiology procedures. It provides contact-force feedback via a visual display on the workstation and vibration feedback on the motion controller.

The Corindus system [17,18] consists of a guidewire driving system and a master console. The system controls a guidewire and a stent. The Corindus system does not offer a haptic feedback function of a guidewire but offers a visual feedback function with a navigation system.

The Amigo robot system [19] consists of a remote controller and a slave robot that controls the insertion, rotation, and steering motion of the catheter. An operator manipulates the catheter using the remote controller. However, the system does not have a haptic feedback function.

Cha et al. [20,21] developed a 4-degree of freedom (DOF) robotic system and a 5-DOF robotic system for vascular intervention. The 4-DOF robotic system controls the guidewire and the catheter, and the 5-DOF robotic system includes a steerable catheter. Both systems offer the haptic feedback function. However, it does not provide any exact information, because the contact force of the guidewire is measured indirectly according to the current of the actuator.

In this study, a previously developed 5-DOF slave robot [21] was used, and a 6-DOF master device was specially designed. Additionally, a steering catheter was designed to conduct vascular intervention surgery. By using the steering catheter and haptic function, the task-time and the repulsive force were significantly reduced compared with the case of a curved catheter.

2. Robotic System for Vascular Intervention

2.1. 5-DOF Slave Robot

This section briefly introduces the 5-DOF slave robot shown in Figure 1. The previous robot for vascular intervention [20] was designed to have 4 DOFs, including insertion and rotation of both the guidewire and catheter. The second design [21] having 5 DOFs included a catheter steering function. The modified version shown in Figure 1 has the same 5 DOFs, but an FT (Force/Torque) sensor is newly installed to measure the interaction force between the catheter and the vascular lines.

The main reason for adding the steerable function to the catheter is to facilitate access to and branching in the blood vessel. The main reason for employing the haptic function is to prevent perforation as the catheter passes through largely curved vascular lines. To measure the force, an FT sensor was used (ROBOTUS, RFT60-HA01 force load capacity (based on z-axis): 200 N; force resolution (based on z-axis): 200 mN; torque load capacity: 4 Nm, torque resolution 5 mNm). The operation principle of FT sensor is capacitance sensing. When the electrode (−) is moved by an external force, it reacts with the electrode (+) fixed on the substrate. Therefore, the FT sensor can measure the magnitude of the external force. The operation principle is well described in [22]. The FT sensor

is installed at the location where the root of the catheter is attached to the body of the slave robot, as shown in Figure 1, and it provides a ground-truth data for the repulsive force measured during the insertion of the catheter.

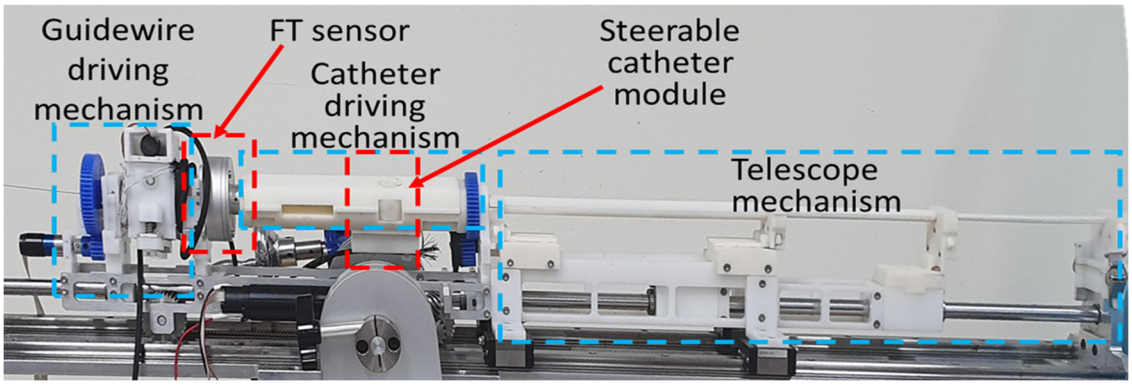

Figure 1. Five degrees of freedom (5-DOF) slave robotic system for vascular intervention.

Conventional catheters used in the operating room are operated by two modes: catheter rotation and catheter insertion. However, it is sometimes difficult to make branching in complex vascular lines with movements of the catheter. For this reason, a steerable-catheter module was employed not only for successful branching but also to reduce the possibility of perforation of the patient's vessel during vascular intervention surgery. The detailed results are discussed in Section 5.

2.1.1. Motion

In this study, the slave robotic system for vascular intervention had a total of 5 DOFs: steering, insertion and rotation of the catheter, and insertion and rotation of the guidewire. This motion mimics the surgeon's motion during a vascular intervention surgery. Figure 2 describes the motion of the slave robot system for vascular intervention.

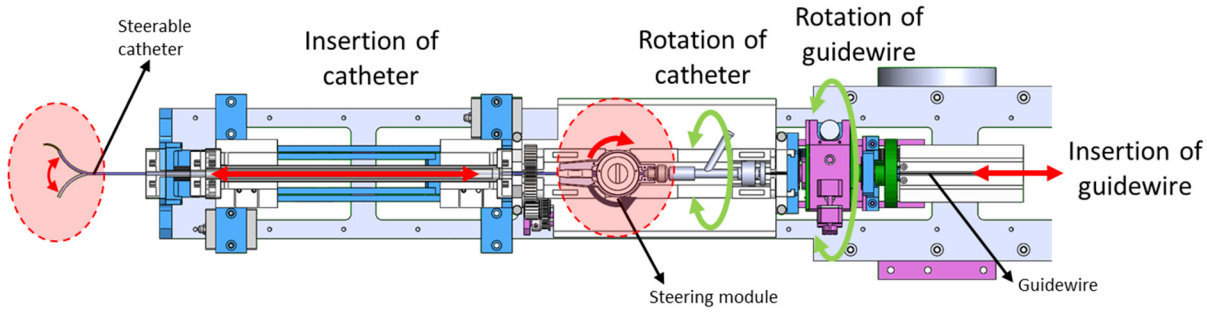

Figure 2. Motions of the 5-DOF slave robot.

2.1.2. Steerable-Catheter Module

The steerable catheter is designed by connecting a soft part and a rigid part, as shown in Figure 3. Two wires pass through the rigid and soft parts and are connected to the distal end of the catheter. The cross-sectional area consists of three holes; two for steering wires and one for the guidewire. Two wires pass through the proximal part of the rigid part and are connected to the spool. By rotating the knob on the spool, a steerable motion of the catheter is generated. When the spool is installed on the slave robot, a stepping motor connected to the spool turns the spool knob for the steering of the catheter, as shown in Figure 4.

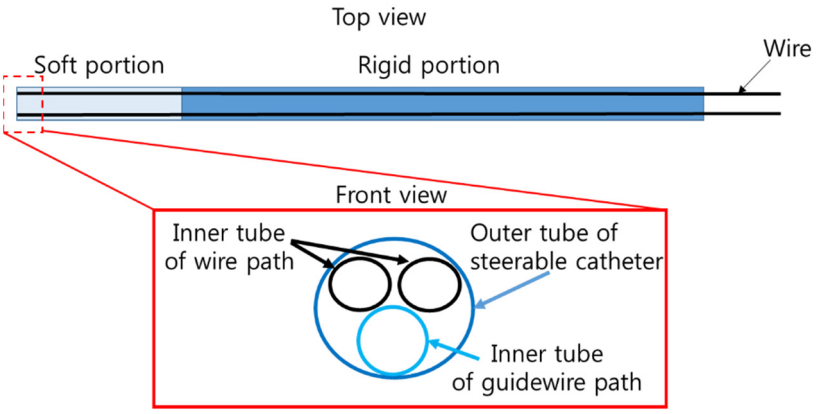

Figure 3. Structure of the steerable catheter.

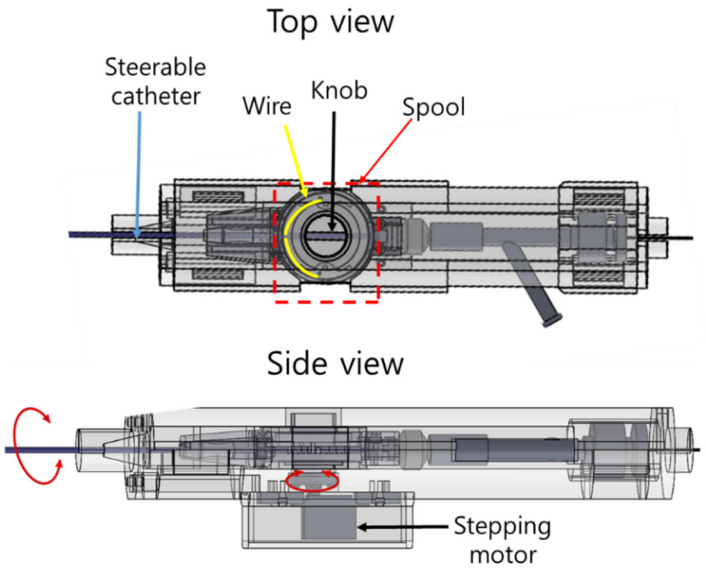

Figure 4. Assembly of the steerable catheter and the spool.

2.2. *Master Device*

The master device for controlling the slave robot must have at least 5 DOFs for insertion, rotation, and steering of the catheter and insertion and rotation of the guidewire. An intuitive design is required, because the motions of the guidewire and catheter are similar. Additionally, a haptic function is needed to make the user feel the repulsive force generated by the blood-vessel wall during the insertion of the catheter. In this paper, we designed a master device that combines a mechanism for 3-DOF x-y-z translational motion and a mechanism for 4-DOF rotational motion. The proposed master device is kinematically redundant. 3-DOF rotational motion is sufficient to perform wrist motion similar to that of a human, but the motion is not natural. Kinematically redundant features help the operator to move more naturally when manipulating the master device. Therefore, to facilitate the operation of the master device, a kinematically redundant master device is proposed.

2.2.1. Structure

As shown in Figure 5, the 3-DOF x-y-z positioning device is constructed by combining a double four-bar structure and a five-bar structure. The 4-DOF mechanism is constructed by combining three-axis rotational motion with one additional redundant DOF and one grip motion, as shown in Figure 6.

Additionally, a foot switch is used to distinguish between catheter control and guidewire control, and the operation of the catheter and guidewire is controlled by one master device through mode

change. The grip switch of Figure 6b allows the user to repeatedly insert the catheter and guidewire through an activating and releasing command.

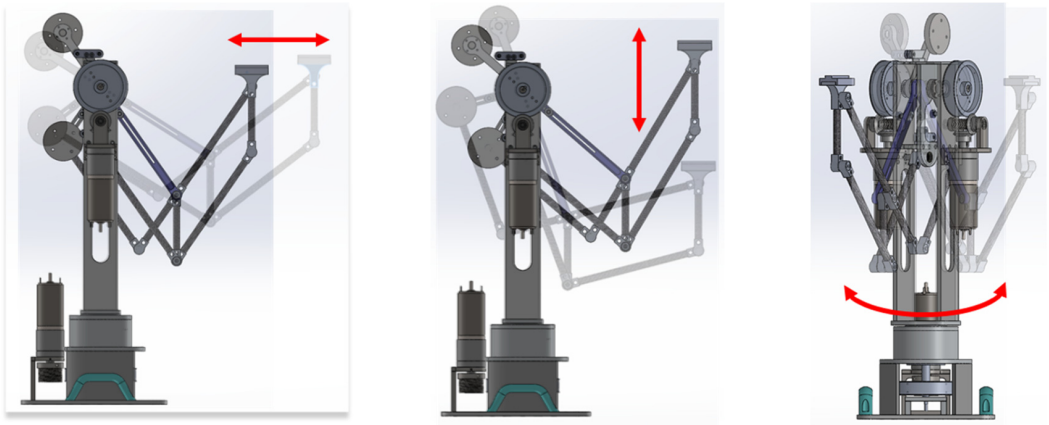

(**a**) (**b**) (**c**)

Figure 5. 3-DOF stackable mechanism: (**a**) *z*-axis; (**b**) *y*-axis; (**c**) *x*-axis.

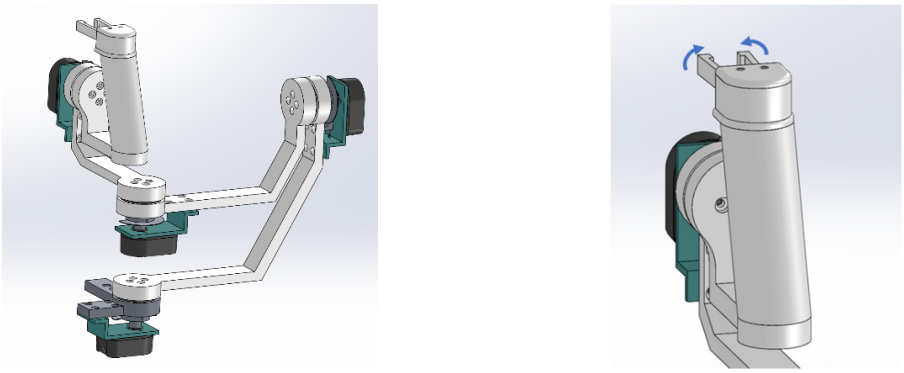

(**a**) (**b**)

Figure 6. 4-DOF wrist mechanism: (**a**) 3-DOF wrist mechanism; (**b**) grip motion.

For the haptic function, a 3-DOF stackable mechanism is equipped with a motor. The user can feel the repulsive force by using the information measured by an FT sensor in the slave robot. The master device system is configured as shown in Figure 7.

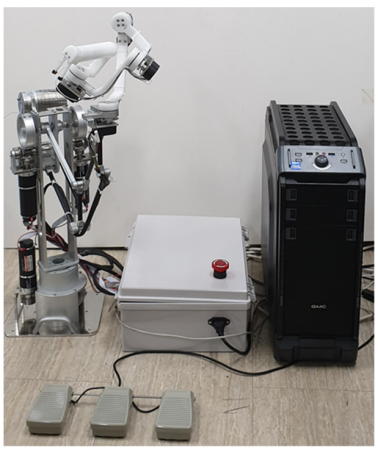

Figure 7. Master device system.

2.2.2. Motion Matching

To operate the slave robot that drives the catheter and the guidewire with the master device, it is necessary to match each motion of the slave robot with the motion of the master. Because the catheter control mode and guidewire control mode can be changed using the footswitch, the master device matches only the insertion and rotation operations of the slave robot regardless of the catheter or guidewire; the steering operation of the steerable catheter is independently controlled. Figure 8 shows that only three axes of the master device are employed for motion matching between the slave robot and master device.

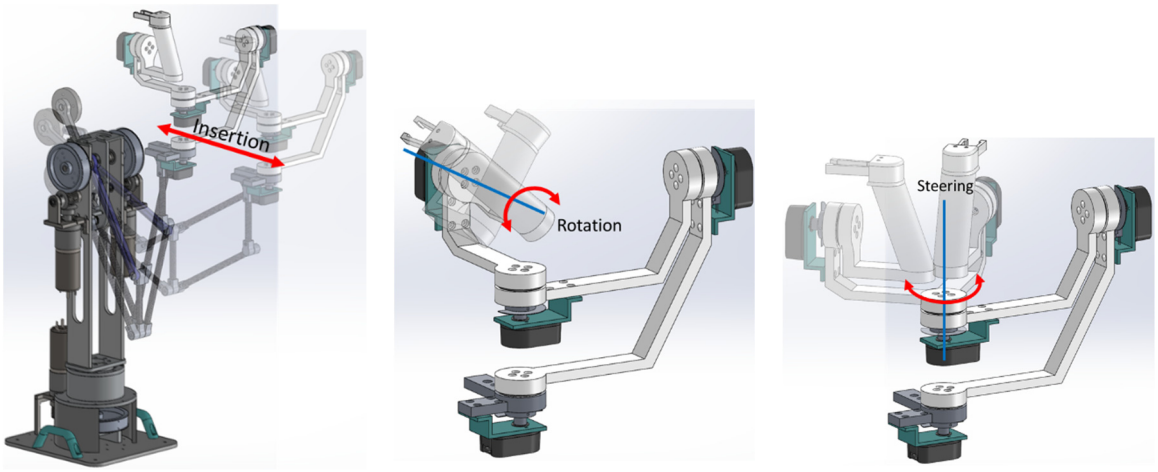

(**a**) (**b**) (**c**)

Figure 8. Motion matching: (**a**) insertion motion; (**b**) rotation motion; (**c**) steering motion.

2.3. Master–Slave System

The master device and the slave robot are controlled through a single personal computer (PC). The PC obtains motion information and mode information from the master device and sends an operation command to the slave robot. The slave robot drives the catheter and the guidewire according to the motion information from the master device. The FT sensor mounted on the slave robot measures the repulsive force generated by the blood-vessel wall while the catheter is being inserted, and the PC sends a haptic command to the master device according to the measured FT sensor value. A block diagram of the master–slave system is shown in Figure 9.

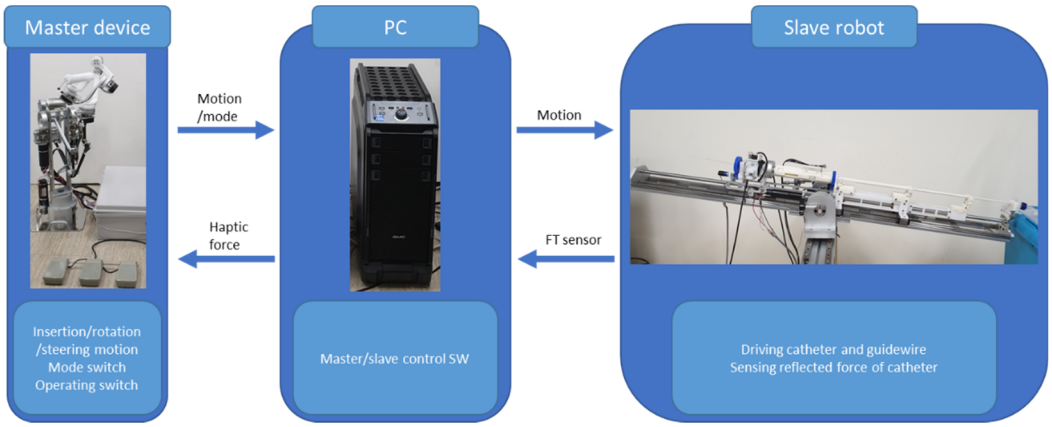

Figure 9. Block diagram of the master–slave system.

3. Experiments

We compared the performance of the existing curved catheter and the developed steerable catheter (Figure 10) for the vascular interventional robotic system. The effectiveness of the haptic function was experimentally tested. The phantom employed in this experiment was manufactured by United Biologics [23]. It was designed to include vascular lines of the abdominal region. The experiment comprised three scenarios, as shown in Table 1. Each scenario targeted three points of the vascular phantom. Figure 11 presents details regarding the three targets and their paths. The path to the first target was smooth compared with those to the other targets. The third target was the most difficult to reach, as the path was highly curved. The operator controlled the slave robot by using the master device with visual feedback from top-view and side-view cameras. For each scenario, the time taken to reach the target and the repulsive force measured during the insertion of the catheters were measured. The experiment was repeated 10 times for each target to obtain average data.

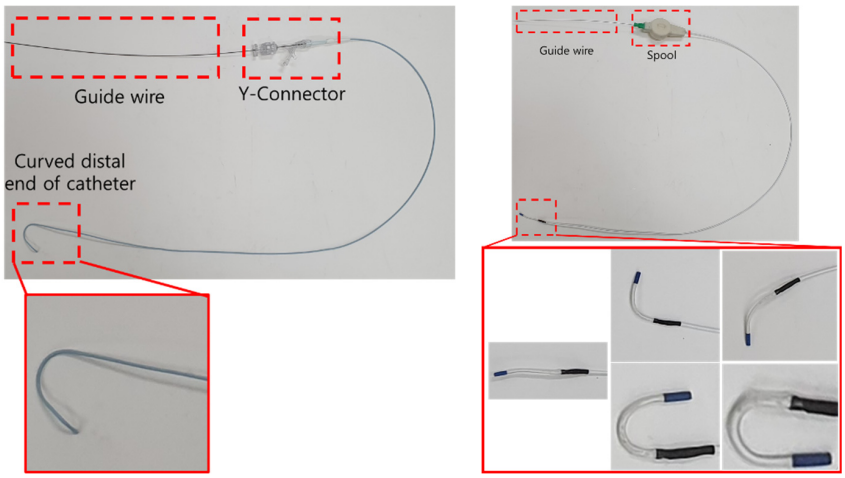

(**a**) (**b**)

Figure 10. (**a**) 5F (1.67 mm) conventional curved catheter; (**b**) 6F (2 mm) steerable catheter.

Table 1. Scenarios.

Scenario	Method
1	Using conventional curved catheter
2	Using steerable catheter
3	Using steerable catheter with haptic function

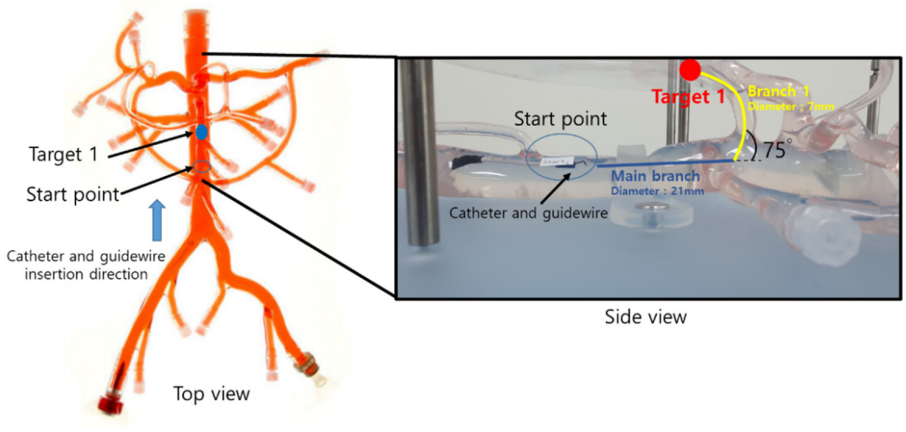

(**a**)

Figure 11. *Cont.*

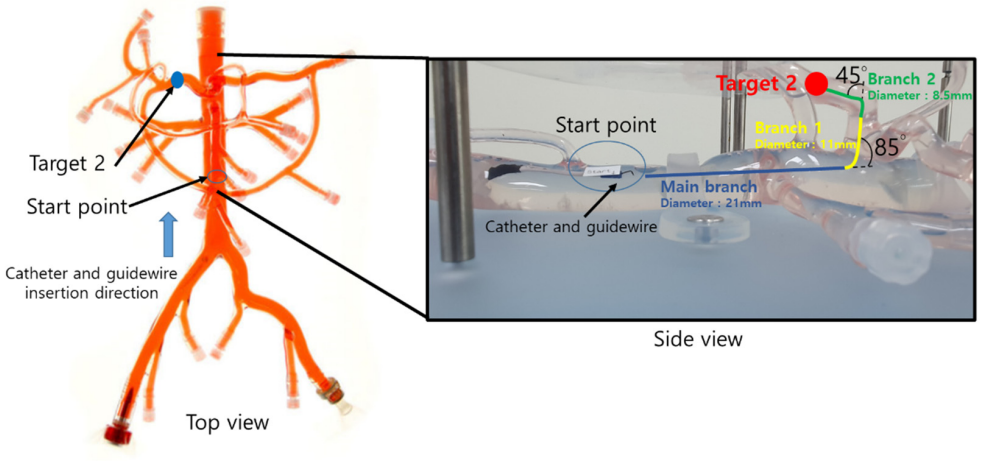

(**b**)

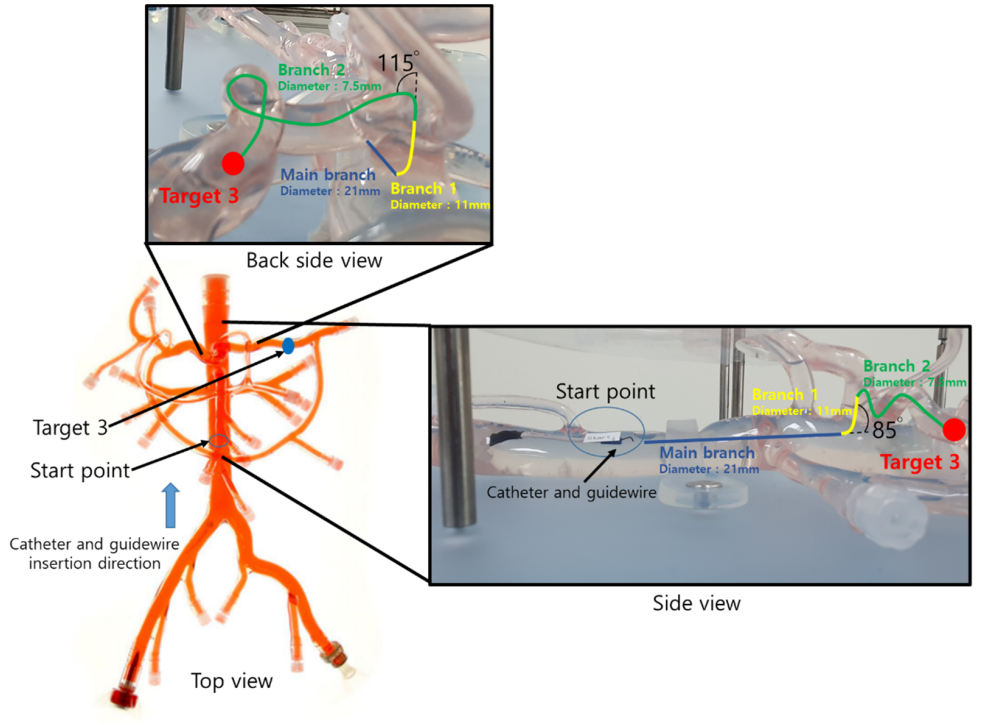

(**c**)

Figure 11. Three target points in the vascular phantom: (**a**) Target 1; (**b**) Target 2; (**c**) Target 3.

3.1. Scenario 1

In Scenario 1, a curved catheter, which is a commercial product, was used. The time taken to reach the three targets and the repulsive force due to interaction with the vessel wall were measured and averaged. Figure 12 presents the experimental results for Scenario 1, which clearly differed among the three targets. For the first target, the task-time was measured as 2 min 41 s, and the average force per second was measured as 0.4226 N. For the second target, the task-time was 2 min 51 s, and the average force per second was 0.7078 N. For the third target, the task-time was 7 min 24 s, and the average force per second was 1.0465 N. The experimental results indicate that the task-time was the longest for Target 3. This is because the branches to Target 3 were more complex than those to the other targets.

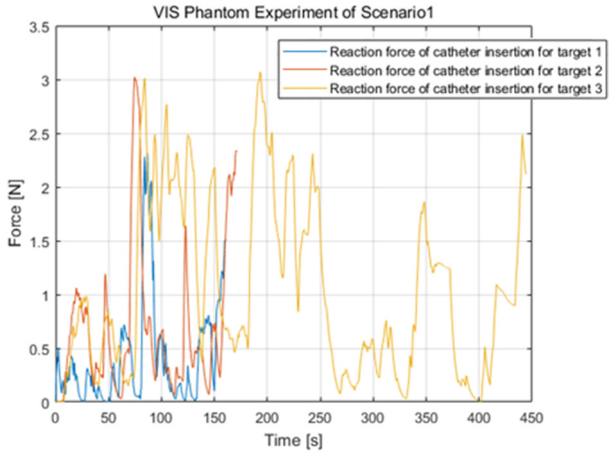

Figure 12. Reaction force for the three different targets in the case of the commercial catheter.

3.2. Scenario 2

Scenario 2 tested the effect of a steerable catheter, i.e., a catheter with a steering function. In the experiment, the time and the force were measured until the three targets were reached, similar to Scenario 1. Figure 13 presents the experimental results for Scenario 2, which clearly differed among the three targets. For the first target, the task-time was 2 min 28 s, and the average force per second was 0.2850 N. For the second target, the task-time was 2 min 11 s, and the average force per second was 0.2015 N. For the third target, the task-time was 3 min and 17 s, and the average force per second was 0.3544 N. Compared with the results for the curved catheter, the task-time and repulsive force were reduced, indicating the effectiveness of the steerable catheter.

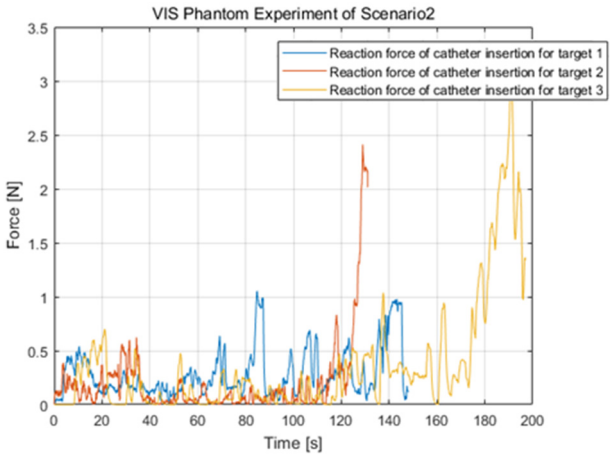

Figure 13. Reaction force for the three different targets in the case of the steerable catheter.

3.3. Scenario 3

In Scenario 3, the steerable catheter was used, but the haptic function was added to allow the user to feel the repulsive force generated by the vessel wall during the insertion of the steerable catheter. This objective of the experiment was to determine whether the haptic function can prevent vascular damage such as perforation. The process was identical to that for the two aforementioned scenarios. Figure 14 presents the experimental results for Scenario 3, clearly indicating the differences among the results for the three targets. For the first target, the task-time was 1 min 22 s, and the average force per second was 0.2188 N. For the second target, the task-time was 1 min 39 s, and the average force per second was 0.1811 N. For the third target, the task-time was 2 min 6 s, and the average force per second was 0.2690 N. With the haptic function, both the task-time and repulsive force were improved, indicating the effectiveness of the haptic function.

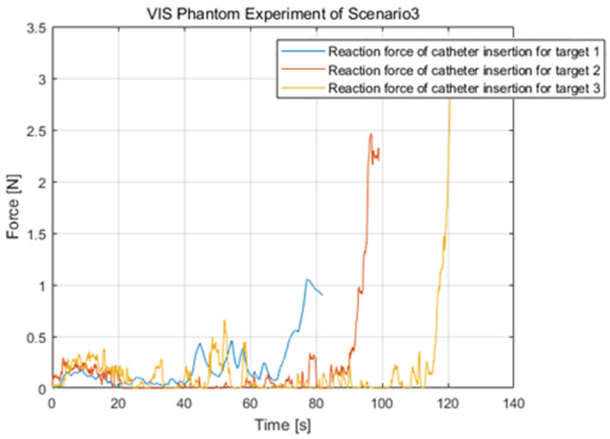

Figure 14. Reaction force for the three different targets in the case of the steerable catheter with the haptic function.

4. Results

The task-time was reduced by using the steerable catheter in Scenario 2 compared with the case of the commercial curved catheter in Scenario 1. Additionally, by applying the haptic function in Scenario 3, the average measured force could be reduced by allowing the user to manipulate the catheter without exerting an excessive force on the vessel wall.

The experimental results for the different targets, which are presented in Table 2 and Figures 15–17, also indicate the following. For Target 1, the task-time was reduced by 8.07% when the steering catheter was used and was reduced by 49.07% when the haptic function was added. Additionally, the average measured force per second was reduced by 32.56% for the steering catheter and was reduced by 48.23% for the haptic function. For the Target 2, the task-time was reduced by 23.39% when the steering catheter was used and was reduced by 42.11% when the haptic function was added. The average force per second was reduced by 71.53% when the steering catheter was used and was reduced by 74.41% when the haptic function was added.

Finally, compared with the case of the conventional curved catheter for Target 3, the task-time for the steering catheter was reduced by 56.98% and was reduced by 71.62% when the haptic function was added. Additionally, the average force per second was reduced by 66.13% when the steering catheter was used and was reduced by 74.30% when the haptic function was added.

Table 2. Experimental results for each target.

Target	Scenario *	Task-Time (s)	Average Force (N)/s
1	1	161	0.4226
	2	148	0.2850
	3	82	0.2188
2	1	171	0.7078
	2	131	0.2015
	3	99	0.1811
3	1	444	1.0465
	2	191	0.3544
	3	126	0.2690

* Scenario 1: only curved catheter; Scenario 2: steerable catheter; Scenario 3: steerable catheter + haptic function.

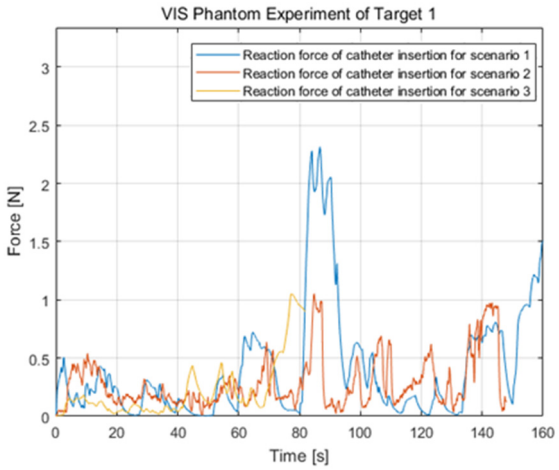

Figure 15. Reaction force in the three different scenarios for Target 1.

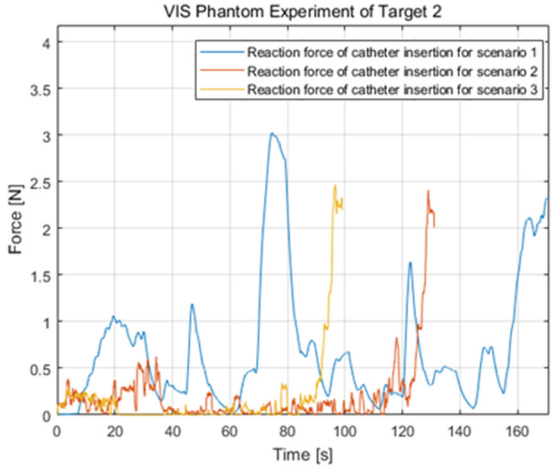

Figure 16. Reaction force in the three different scenarios for Target 2.

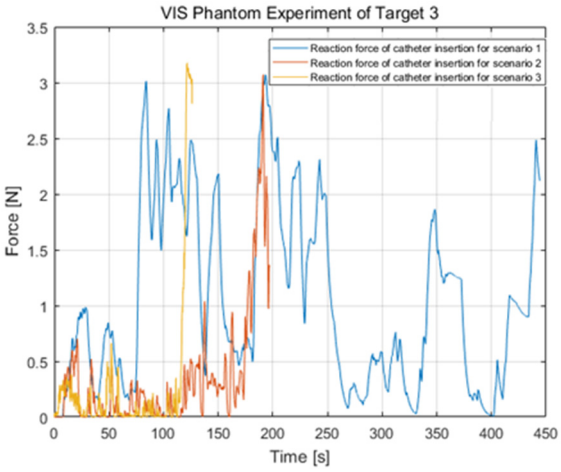

Figure 17. Reaction force in the three different scenarios for Target 3.

5. Discussion

We examined the effectiveness of a steering catheter and a haptic function in the vascular intervention procedure. A 5-DOF vascular interventional robot system and a 7-DOF master device were employed for a blood-vessel phantom experiment. The experimental results indicated that the haptic feedback and steerable catheter were useful for reducing the procedure time and minimizing

the damage to the vessel wall. Therefore, applying the steerable catheter and haptic feedback during vascular intervention can reduce the radiation dose to the patient, as well as the vascular perforation. The proposed 5-DOF vascular interventional robot system and 7-DOF master device can assist inexperienced surgeons to easily drive catheters and guidewires in vascular intervention. When the catheter and guidewire must pass through complex blood vessels, manipulating them is difficult for inexperienced surgeons. By using our proposed robot, inexperienced surgeons can easily access difficult vessels with a steerable catheter and haptic feedback. Regarding safety, the insulation problem should be resolved in accordance with IEC60601-1 3.1ed. Adding more sensors to the final commercial product is not recommended. Instead of using a force/torque sensor, the interaction force can be indirectly measured according to the current change in the motor controller. The application areas of this device are diverse, including chemotherapy for liver cancer and stent installation on the heart.

Many future studies related to this research can be performed. In recent studies, various sensors and artificial intelligence were applied to surgical robots [24–26]. In the present study, force measurements using the FT sensor were performed only on the catheters. This is because the catheter contacted most of the vascular line, while only the distal part of the guidewire contacted the vascular line. However, it is necessary to measure the repulsive force induced by the guidewire, particularly when the vascular line is already closed. Recently, research has been conducted on the use of deep neural networks in a vascular interventional robot. Research is also being performed to predict the force generated during vascular intervention according to the motor current data by using deep neural networks instead of an FT sensor. The force measured by an FT sensor can be initially used as the ground truth, but the FT sensor can be removed once the learning process is complete. In the future, it is expected that the degree of autonomy in robotic vascular intervention can be increased. W. Chi et al. [27] reported vascular intervention path planning using reinforcement learning. Similarly, we plan to apply a reinforced learning algorithm to our vascular intervention robotic system for successful insertion of the catheter into the vascular lines. Precise haptic rendering is another important research topic [28].

Author Contributions: J.W. and H.-S.S. contributed to the software and experiments, acquired the data, analyzed the data, and wrote the paper; H.-J.C. contributed to the paper review and editing; and B.-J.Y. contributed to the supervision, project administration, and review and editing. All the authors contributed to the paper.

Funding: This work was supported by the Technology Innovation Program (or Industrial Strategic Technology Development Program-Artificial intelligence bio-robot medical convergence project) (20001257, Artificial intelligence algorithm based vascular intervention robot system for reducing radiation exposure and achieving 0.5 mm accuracy) funded by the Ministry of Trade, Industry & Energy (MOTIE, Korea), the Ministry of Health & Welfare (MOHW), Ministry of Science and ICT (MSIT), and the Korea Evaluation Institute of Industrial Technology (KEIT).

Conflicts of Interest: The authors declare no conflict of interest.

References

1. Koh, T.K.; Ting, J.Z.L.; Wee, B.; Khamitov, R.; Teoh, K.; Wong, J.; Sorokin, V.A. Coronary and arch hybrid surgery in a patient with infrarenal aortic occlusion. *Asian Cardiovasc. Thorac. Ann.* **2018**, *26*, 148–150. [CrossRef]
2. Blehm, A.; Sorokin, V.A.; Hartman, M.; Wai, K.L.; Schmitz, K.; Lichtenberg, A. Quality of Life Shift after Aortic Valve Replacement in the Era of TAVI: Single-Center Class Comparison Study Between Different Procedural Techniques. *J. Heart Valve Dis.* **2015**, *24*, 540–553.
3. Vickneson, K.; Chan, S.P.; Li, Y.; Bin MA, A.; Luo, H.D.; Kang, G.S.; Sorokin, V. Coronary artery bypass grafting in patients with low ejection fraction: What are the risk factors? *J. Cardiovasc. Surg.* **2019**, *60*, 396–405. [CrossRef]
4. Pantos, I.; Patatoukas, G.; Katritsis, D.G.; Efstathopoulos, E. Patient radiation doses in interventional cardiology procedures. *Curr. Cardiol. Rev.* **2009**, *5*, 1–11. [CrossRef] [PubMed]
5. Efstathopoulos, E.P.; Pantos, I.; Andreou, M.; Gkatzis, A.; Carinou, E.; Koukorava, C.; Kelekis, N.L.; Brountzos, E. Occupational radiation doses to the extremities and the eyes in interventional radiology and cardiology procedures. *Br. J. Radiol.* **2011**, *84*, 70–77. [CrossRef] [PubMed]

6. Mohapatra, A.; Greenberg, R.K.; Mastracci, T.M.; Eagleton, M.J.; Thornsberry, B. Radiation exposure to operating room personnel and patients during endovascular procedures. *J. Vasc. Surg.* **2013**, *58*, 702–709. [CrossRef] [PubMed]
7. Vaño, E.; Gonzalez, L.; Fernandez, J.M.; Alfonso, F.; Macaya, C. Occupational radiation doses in interventional cardiology: A 15-year follow-up. *Br. J. Radiol.* **2006**, *79*, 383–388. [CrossRef]
8. Goni, H.; Papadopoulou, D.; Yakoumakis, E.; Stratigis, N.; Benos, J.; Siriopoulou, V.; Makri, T.; Georgiou, E. Investigation of occupational radiation exposure during interventional cardiac catheterisations performed via radial artery. *Radiat. Prot. Dosim.* **2005**, *117*, 107–110. [CrossRef]
9. Miller, D.L.; Balter, S.; Cole, P.E.; Lu, H.T.; Schueler, B.A.; Geisinger, M.; Cardella, J.F. Radiation doses in interventional radiology procedures: The RAD-IR study: Part I: Overall measures of dose. *J. Vasc. Interv. Radiol.* **2013**, *14*, 711–727. [CrossRef]
10. Wrixon, A.D. New ICRP recommendations. *J. Radiol. Prot.* **2008**, *28*, 161–168. [CrossRef]
11. Kong, C.H.; Lin, X.Y.; Woo, C.C.; Wong, H.C.; Lee, C.N.; Richards, A.M.; Sorokin, V.A. Characteristics of aortic wall extracellular matrix in patients with acute myocardial infarction: Tissue microarray detection of collagen I, collagen III and elastin levels. *Interact. Cardiovasc. Thorac. Surg.* **2012**, *16*, 11–15. [CrossRef] [PubMed]
12. Chiong, T.; Cheow, E.S.; Woo, C.C.; Lin, X.Y.; Khin, L.W.; Lee, C.N.; Sorokin, V.A. Aortic Wall Extracellular Matrix Proteins Correlate with Syntax Score in Patients Undergoing Coronary Artery Bypass Surgery. *Open Cardiovasc. Med. J.* **2016**, *10*, 48–56. [CrossRef] [PubMed]
13. Woo, J.; Choi, J.H.; Seo, J.T.; Kim, T.I.; Yi, B.J. Development of a robotic colonoscopic manipulation system, using haptic feedback algorithm. *Yonsei Med J.* **2017**, *58*, 139–143. [CrossRef] [PubMed]
14. Antoniou, G.A.; Riga, C.V.; Mayer, E.K.; Cheshire, N.J.; Bicknell, C.D. Clinical applications of robotic technology in vascular and endovascular surgery. *J. Vasc. Surg.* **2011**, *53*, 493–499. [CrossRef] [PubMed]
15. Hansen Medical. Available online: http://www.hansenmedical.com/ (accessed on 9 November 2017).
16. Saliba, W.; Cummings, J.E.; Oh, S.; Zhang, Y.; Mazgalev, T.N.; Schweikert, R.A.; Burkhardt, D.; Natale, A. Novel robotic catheter remote control system: Feasibility and safety of transseptal puncture and endocardial catheter navigation. *J. Cardiovasc. Electrophysiol.* **2006**, *17*, 1102–1105. [CrossRef]
17. Rafael, B.; Luis, G.; Dan, D.; Ariel, R.; Yaron, A.; Silviu, C.; Ganesh, K.; Tal, W. Remote-control percutaneous coronary interventions: Concept, validation, and first-in-human pilot clinical trial. *J. Am. Coll. Cardiol.* **2006**, *47*, 296–300.
18. Juan, F.G.; Juan, A.D.; Maria, P.U.; Andres, F.; Guillermo, B.; Martin, B.L.; Giora, W. First-in-human evaluation of a novel roboticassisted coronary angioplasty system. *JACC Cardiovasc. Interv.* **2011**, *4*, 460–465.
19. Khan, E.M.; Frumkin, W.; Ng, G.A.; Neelagaru, S.; Abi-Samra, F.M.; Lee, J.; Giudici, M.; Gohn, D.; Winkle, R.A.; Sussman, J.; et al. First experience with a novel robotic remote catheter system: AmigoTM mapping trial. *J. Interv. Card. Electrophysiol.* **2013**, *37*, 121–129. [CrossRef]
20. Cha, H.-J.; Yi, B.-J.; Won, J.Y. An assembly-type master-slave catheter and guidewire driving system for vascular intervention. *Proc. Inst. Mech. Eng. H. J. Eng. Med.* **2017**, *231*, 69–79. [CrossRef]
21. Cha, H.-J.; Yoon, H.-S.; Jung, K.Y.; Yi, B.-J.; Lee, S.; Won, J.Y. A robotic system for percutaneous coronary intervention equipped with a steerable catheter and force feedback function. In Proceedings of the IEEE/RSJ International Conference on Intelligent Robots and Systems, Daejeon, Korea, 9–14 October 2016; pp. 1151–1156.
22. Kim, U.; Lee, D.; Kim, Y.B.; Seok, D.; Choi, H.R. A Novel Six-Axis Force/Torque Sensor for Robotic Applications. *IEEE/ASME Trans. Mechatron.* **2017**, *22*, 1381–1391. [CrossRef]
23. Available online: https://unitedbiologics.com/product/abdominal-region/ (accessed on 11 August 2019).
24. Radó, J.; Dücső, C.; Földesy, P.; Bársony, I.; Rohr, K.L.M.; Lis, K.; Sadowski, W.; Krawczyk, D.; Kroczek, P.; Małota, Z.; et al. Biomechanical tissue characterization by force sensitive smart Laparoscope of Robin heart surgical robot. *Proc. Eurosensor* **2018**, *2*, 1035. [CrossRef]
25. Santos, L.; Carbonaro, N.; Tognetti, A.; González, J.L.; de la Fuente, E.; Fraile, J.C.; Pérez-Turiel, J. Dynamic gesture recognition using a smart glove in hand-assisted Laparoscopic surgery. *Technologies* **2018**, *6*, 8. [CrossRef]
26. Xue, R.; Ren, B.; Huang, J.; Yan, Z.; Du, Z. Design and evaluation of FBG-based tension sensor in Laparoscope surgical robots. *Sensors* **2018**, *18*, 2067. [CrossRef] [PubMed]

27. Chi, W.; Liu, J.; Abdelaziz, M.E.; Dagnino, G.; Riga, C.; Bicknell, C.; Yang, G.Z. Trajectory optimization of robot-assisted endovascular catheterization with reinforcement learning. In Proceedings of the IEEE/RSJ International Conference on Intelligent Robots and Systems, Madrid, Spain, 1–5 October 2018; pp. 3875–3881.
28. Amirkhani, S.; Bahadorian, B.; Nahvi, A.; Chaibakhsh, A. Stable haptic rendering in interactive virtual control laboratory. *Intell. Serv. Robot.* **2018**, *11*, 289–300. [CrossRef]